

The impact of chemical lateral boundary conditions on CMAQ predictions of tropospheric ozone over the continental United States

Youhua Tang · Pius Lee · Marina Tsidulko · Ho-Chun Huang · Jeffery T. McQueen · Geoffrey J. DiMego · Louisa K. Emmons · Robert B. Pierce · Anne M. Thompson · Hsin-Mu Lin · Daiwen Kang · Daniel Tong · Shaocai Yu · Rohit Mathur · Jonathan E. Pleim · Tanya L. Otte · George Pouliot · Jeffrey O. Young · Kenneth L. Schere · Paula M. Davidson · Ivanka Stajner

Received: 28 February 2008 / Accepted: 10 August 2008
© Springer Science+Business Media B.V. 2008

Abstract A sensitivity study is performed to examine the impact of lateral boundary conditions (LBCs) on the NOAA-EPA operational Air Quality Forecast Guidance over continental USA. We examined six LBCs: the fixed profile LBC, three global LBCs, and two ozonesonde LBCs for summer 2006. The simulated results from these six runs are compared to IONS ozonesonde and surface ozone measurements from August 1 to 5, 2006. The choice of LBCs can affect the ozone prediction throughout the domain, and mainly influence the predictions in upper altitude or near inflow boundaries, such as US west coast and the northern border. Statistical results shows that the use of global model predictions for LBCs could improve the correlation coefficients of surface ozone prediction over the US west coast, but could also increase the ozone mean bias in most regions of the domain depending on global models. In this study, the use of the MOZART (Model for Ozone And Related chemical

Y. Tang · P. Lee · M. Tsidulko · H.-C. Huang
Scientific Applications International Corporation, Camp Springs, MD, USA

Y. Tang (✉) · J. T. McQueen · G. J. DiMego
NOAA/NWS/NCEP/EMC, W/NP22 Room 207, 5200 Auth Road, Camp Springs, MD 20746-4304, USA
e-mail: youhua.tang@noaa.gov

L. K. Emmons
National Center for Atmospheric Research, Boulder, CO, USA

R. B. Pierce
NOAA/NESDIS Advanced Satellite Products Branch, Madison, WI, USA

A. M. Thompson
Department of Meteorology, Pennsylvania State University, University Park, PA, USA

H.-M. Lin · D. Kang · D. Tong · S. Yu
Science and Technology Corporation, Hampton, VA, USA

R. Mathur · J. E. Pleim · T. L. Otte · G. Pouliot · J. O. Young · K. L. Schere
EPA National Exposure Research Laboratory, Research Triangle Park, NC, USA

P. M. Davidson
Office of Science and Technology, NOAA/National Weather Service, Silver Spring, MD, USA

I. Stajner
Noblis Inc, Falls Church, VA, USA

Tracers) prediction for CMAQ (Community Multiscale Air Quality) LBC shows a better surface ozone prediction than that with fixed LBC, especially over the US west coast. The LBCs derived from ozonesonde measurements yielded better O_3 correlations in the upper troposphere.

Keywords Air quality model · CMAQ · Boundary condition · Ozonesonde · AIRNOW · Chemical transport model · Ozone prediction

1 Introduction

The National Air Quality Forecast Guidance (NAQFG) run at the United States' National Centers for Environmental Prediction (NCEP) [13, 20] uses time-invariant profiles as the chemical lateral boundary conditions (LBCs) for air quality predictions over the continental United States. The profile LBCs are often used even in retrospective air quality modeling when influences of transport outside of a limited modeling domain are relatively weak compared to the impact of emissions within the model domain. Over the continental United States, the major inflows are seasonal and sporadic such as pollutants emitted from Asia transported across the Pacific which are usually enhanced during springtime [7, 8], pollutants from Mexico that affect the southern border, and northern influx from Canadian emissions, and occasionally Canadian and Alaskan wildfire plumes (e.g., [12]) and Saharan dust. The static LBCs obviously cannot reflect the chemical influences related to intermittent events. Here, we explore alternative approaches to defining the chemical LBCs for the NAQFG, including LBCs derived from global model predictions and from observational data, with the goal of better capturing the day-to-day variability in the chemical fields to provide improved ozone forecasts. In this study, we do not test the top boundary condition as [32] and CMAQ currently uses gradient-zero top boundary conditions. If at the top layer the vertical velocity is upward, it is just an outflow and no LBC is needed. For cases when there an inflow (downward motion), we just use the concentration at the top-most layer to estimate in advective flux in.

2 Models and lateral boundary conditions

The NOAA-EPA NAFQS is based on a one-way “offline” coupling of the North American Mesoscale (NAM) Model, which is currently the Weather Research and Forecasting Model–Non-hydrostatic Mesoscale Model (WRF-NMM; [11]), and Community Multiscale Air Quality (CMAQ) Modeling System [1]. The NAM is run for the full North American continent on a latitude–longitude domain with ~ 12 -km horizontal grid spacing, and it contains 60 sigma-pressure hybrid layers up to 2 hPa. The primary physics options in the NAM include the NOAA (NOAA/Oregon State/AFWA /Office of Hydrology-NWS) unified 5-layer land and surface model [2], the Mellor–Yamada–Janjic planetary boundary layer (PBL) closure scheme [10], Ferrier cloud microphysics [3] and the Betts–Miller–Janjic convective mixing scheme [9]. In the NAQFG, CMAQ is run over the continental United States with 12-km horizontal grid spacing and uses 22 common WRF-NMM terrain following vertical layers from surface to 100 hPa. The CMAQ model employs the Carbon Bond 4 (CB4) chemical mechanism [4], vertical diffusivity and dry deposition based on [26], scale J-table for photolysis attenuation due to cloud, and Asymmetric Convective Model for the PBL (ACM2) [25]. The National Emission Inventory (NEI) with base year 2001 with recent updated point

Table 1 Global models and their configurations in this study

	MOZART	RAQMS	GFS O ₃
Horizontal Resolution	2.8° × 2.8°	2° × 2°	0.31° × 0.31°
Meteorology	GFS analysis	GFS analysis	GFS forecasts
Anthropogenic emissions	[5]	GEIA/EDGAR inventory with updated Asian emission [30]	Not applicable
Biomass burning emissions	GFED-v2 [35]	Ecosystem/severity based	Not applicable
Stratospheric ozone	Synthetic ozone constraint [16]	OMI/TES assimilation [24]	Initialized by SBUV-2

and mobile emissions is used in this study. We use biogenic Emission Inventory System (BEIS) version 3.13 [22] to generate hourly biogenic emissions for the model simulations. Additional details on the NAQFG configuration can be found in [20] and [14].

In this study, six simulations are conducted with the NAQFG to assess the impacts of various sources of LBCs. The first simulation, “Fixed LBCs”, uses the time-invariant chemical profile LBCs that are employed in the operational system. Three additional simulations are performed to assess the impact of using LBCs derived from global models (Table 1) for the time-varying chemical boundary conditions. These global models incorporate satellite-based chemical data, but with different methodologies. Among the global models, the Model for Ozone And Related chemical Tracers (MOZART) model (version 4, updated from [6]) has the most detailed reactions and related chemical species (97 species), including bulk sulfate, ammonium, organic and soot aerosols, and size-resolved dust and sea salts (e.g., [21]). The Real-time Air Quality Modeling System (RAQMS) [23] model used in this study has only gaseous chemistry. A statistical digital filter analysis system [28,29] was used in RAQMS data assimilation to perform a univariate assimilation of stratospheric profile and total column ozone observations from Aura OMI (Ozone Monitoring Instrument) satellite data [24]. In the simulations with LBCs derived from MOZART and RAQMS fields, the time-varying chemical LBCs include full-profile O₃, CO, sulfur oxidants, nitrogen oxidants and volatile organic compounds (VOCs). Table 2 shows the species mapping tables which is used to convert the LBC species concentrations of RAQMS and MOZART to CMAQ’s implementation of CB4. MOZART and RAQMS have similar inorganic gaseous species. RAQMS’s mechanism is modified from CB4 by including explicitly treated ethane (C₂H₆) and a different lumping method for alkenes. The MOZART chemical mechanism has more explicit VOCs, which are simply split into paraffin (PAR) and olefin (OLE) carbon bonds. The third simulation initializes CMAQ LBCs with 3D prognostic O₃ fields from NCEP’s operational Global Forecast System (GFS) [17,18]. The O₃ prediction in GFS is initialized from assimilation of Solar Backscatter Ultra-Violet (SBUV-2) satellite observations, and O₃ is advected as a trace species with simple zonally averaged climatological derived production and depletion mechanism [27]. Since SBUV-2 can only provide O₃ data above 250hPa, GFS-O₃ LBC is applied to the CMAQ simulation above 11 km, and time-invariant chemical boundary conditions are used for O₃ below 11 km and for all other chemical species. In this study, we import GFS-O₃ LBC every hour while MOZART and RAQMS LBCs are updated every 3 and 6h, respectively.

Table 2 Hydrocarbon species mapping tables between RAQMS and MOZART species and CMAQ CB4

RAQMS species	CMAQ CB4
C2H6	2*PAR
OLET (terminal alkenes)	OLE1 + PAR
OLEI (internal alkenes)	OLE2 + 2*PAR
MOZART species	CMAQ CB4
CH3CHO	ALD2
C2H6	2*PAR
C3H8	3*PAR
BIGALK (higher alkanes)	4*PAR
C3H6	OLE + 2*PAR
BIGENE (higher alkenes)	OLE + 3*PAR
C10H16 (terpene)	OLE + 9*PAR

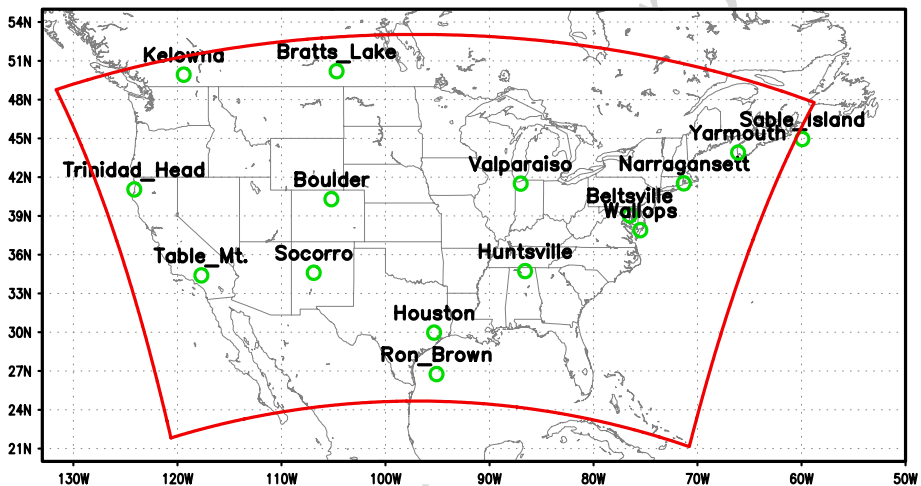


Fig. 1 IONS ozonesonde sites during August 1–5, 2006, and the model domain

87 The final two simulations in this study include the ozone boundary conditions derived
 88 from ozonesondes (see Fig. 1 for the station locations) from the INTEX Ozonesonde Network
 89 Study (IONS; available online at <http://croc.gsfc.nasa.gov/intexb/ions06.html>; [33, 34]) ave-
 90 raged from August 1 to 5, 2006 as the IONS data are not available on earlier dates from
 91 which the simulations started. The IONS balloon-borne ozonesonde data were sampled by
 92 electrochemical concentration cell sensors with an accuracy of about 10% in the troposphere,
 93 but that accuracy can degrade to 15% when O_3 is lower than 10ppbv [19]. For the first of
 94 these simulations, “IONS-LBC1”, the values from the nearest ozonesondes (based on lati-
 95 tude or longitude) to each boundary are assigned and distributed without spatial interpolation
 96 along the lateral boundaries (11 of total 15 ozonesonde sites were used). For example, the
 97 IONS ozonesonde profiles from Table Mountain, Trinidad Head, and Kelowna (Fig. 1) are
 98 distributed from south-to-north (Fig. 2). It should be noted that NOAA Research Ship Ron
 99 Brown (Fig. 1) was not anchored in the same location for this study, so its influence along
 100 the southern boundary varies as a function of its location in the Gulf of Mexico. In the last
 101 of these simulations, “IONS-LBC2”, only the western boundary, a major inflow boundary,

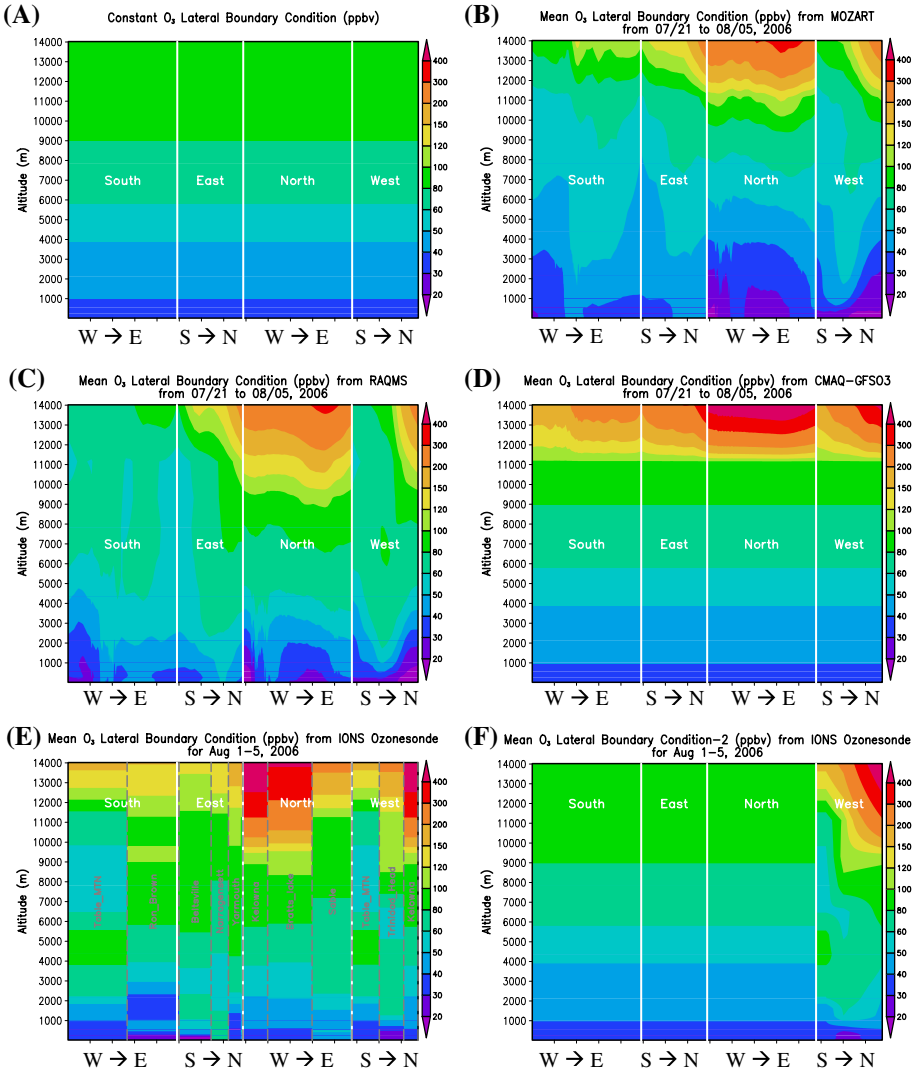


Fig. 2 Mean O₃ lateral boundary conditions along the boundaries of CMAQ 442 × 265 (12-km horizontal grid spacing) CONUS domain. The values are list from west to east for northern and southern boundaries, and from south to north for western and eastern boundaries

102 is changed. In this case, the ozone observations are interpolated (rather than assigned, as
 103 in IONS-LBC1) to the boundary cells. For the boundary cells south of Table Mountain and
 104 cells north of Kelowna, the assignments used in IONS-LBC1 are applied. On the other three
 105 lateral boundaries, the fixed chemical LBCs are used.

106 The simulations in this study are initialized with the CMAQ operational prediction at
 107 12 UTC 21 July 2006 and run for 16 days, driven by daily updated WRF-NMM prediction
 108 initialized at 12 UTC of each day. The simulation period of July 21 to August 5, 2006 includes
 109 several near-surface high-ozone events due to regional and local photochemical activities.
 110 It is neither a particularly strong inflow period, nor a typical scenario for Asian pollutants

111 or biomass burning plumes to reach North America. During the summertime, the long-time
112 (>4 days) trans-Pacific transport cannot bring plumes of short-lived NO_x , SO_x or very active
113 VOCs [31] to North America. Relatively long-lived CO could show some impact if the air
114 mass encountered sufficient NO_x during daytime. However, as more comprehensively studied
115 by [32], the influence of CO on O_3 is one order of magnitude weaker than the influence
116 of O_3 on O_3 in per mole base. So we mainly focus on varying the ozone lateral boundary
117 conditions in this scenario. All the lateral boundary conditions for the sensitivity simulations
118 are implemented throughout the simulation period.

119 Figure 2 shows the mean O_3 LBCs from July 21 to August 5, 2006. Above 11 km, GFS
120 O_3 LBC has the highest mean O_3 concentration. RAQMS and MOZART provide similar O_3
121 LBCs in the upper troposphere, while the major difference appears in the middle troposphere
122 as the RAQMS has more highly concentrated ozone bands extended from upper layers to
123 lower layers. Below 1 km, RAQMS and MOZART have lower mean O_3 LBC than the fixed
124 LBCs.

125 3 Comparison to ozonesondes

126 Ozone predictions from the NAQFG with different chemical LBCs are compared with ozone-
127 sondes from IONS (see Fig. 1). Figure 3 shows the model predictions compared to ozonesonde
128 measurements at six sites on August 3, 2006. At Beltsville, Maryland, all six simulations
129 overpredicted the near-surface O_3 by 10–20 ppbv. The fixed, MOZART, and RAQMS LBCs
130 led to significant underpredictions of the tropospheric O_3 above 4 km and by as much as
131 ~ 50 ppbv above 9 km. Use of the GFS and the ozonesonde-derived LBCs improved the O_3
132 predictions aloft. The IONS LBC1 simulation yielded the best performance over Beltsville,
133 although the fluctuations in the vertical (e.g., between 4 and 9 km) are not captured in any of
134 the simulations due to coarse NAQFG vertical resolution aloft. At Huntsville, Alabama and
135 Boulder, Colorado, GFS O_3 LBC and two IONS LBCs also yielded higher O_3 concentration
136 at high altitudes (e.g., above 6 km) than the simulations with the “fixed”, MOZART, and
137 RAQMS LBCs. However at Boulder, the use of GFS O_3 LBC continued to overestimate O_3
138 above 7 km by 20–30 ppbv, which was much higher than any of the other five methods. Below
139 6 km at Boulder, differences among the simulations except for the IONS LBCs are less than
140 10 ppbv, and the ozonesonde-derived LBCs tend to overpredict O_3 between 4 and 6 km. At
141 Trinidad Head, California, near the domain’s western boundary, using RAQMS LBC and two
142 IONS LBCs resulted in better agreement than the other methods between 1 and 6 km, while
143 the other simulations are about 20 to 40 ppbv lower than the observations at those altitudes.

144 At Bratt’s Lake, Saskatchewan, Canada, which is near the model’s northern boundary, all
145 simulations have comparably good O_3 prediction below 4 km. Above 10 km, a significant
146 ozone intrusion of more than 400 ppbv is observed, which did not appear at the ozonesonde
147 sites except Kelowna on August 3. Here, the importance of using day-specific LBCs is
148 demonstrated as most experiments yield higher and more accurate ozone predictions aloft
149 than using a static profile. In fact, using the ozonesonde data on the lateral boundaries enabled
150 the NAQFG to better capture the ozone enhancement when the balloon entered stratosphere,
151 though it still under predicts the peak values near 12 km by more than 100 ppbv. Winds at
152 Bratt’s Lake were westerly at the time of the observation (Fig. 4a), and hence the source of
153 the increased ozone at Bratt’s Lake likely came from the western boundary, further evidence
154 in the comparison of IONS-LBC1 and IONS-LBC2 at Bratt’s Lake. The observed O_3 aloft at
155 Kelowna, Canada (Fig. 3f) is ~ 400 ppbv, which suggests that the ozone peak at Bratt’s Lake
156 may have originated from an earlier, transient event under westerly wind (Fig. 4) because

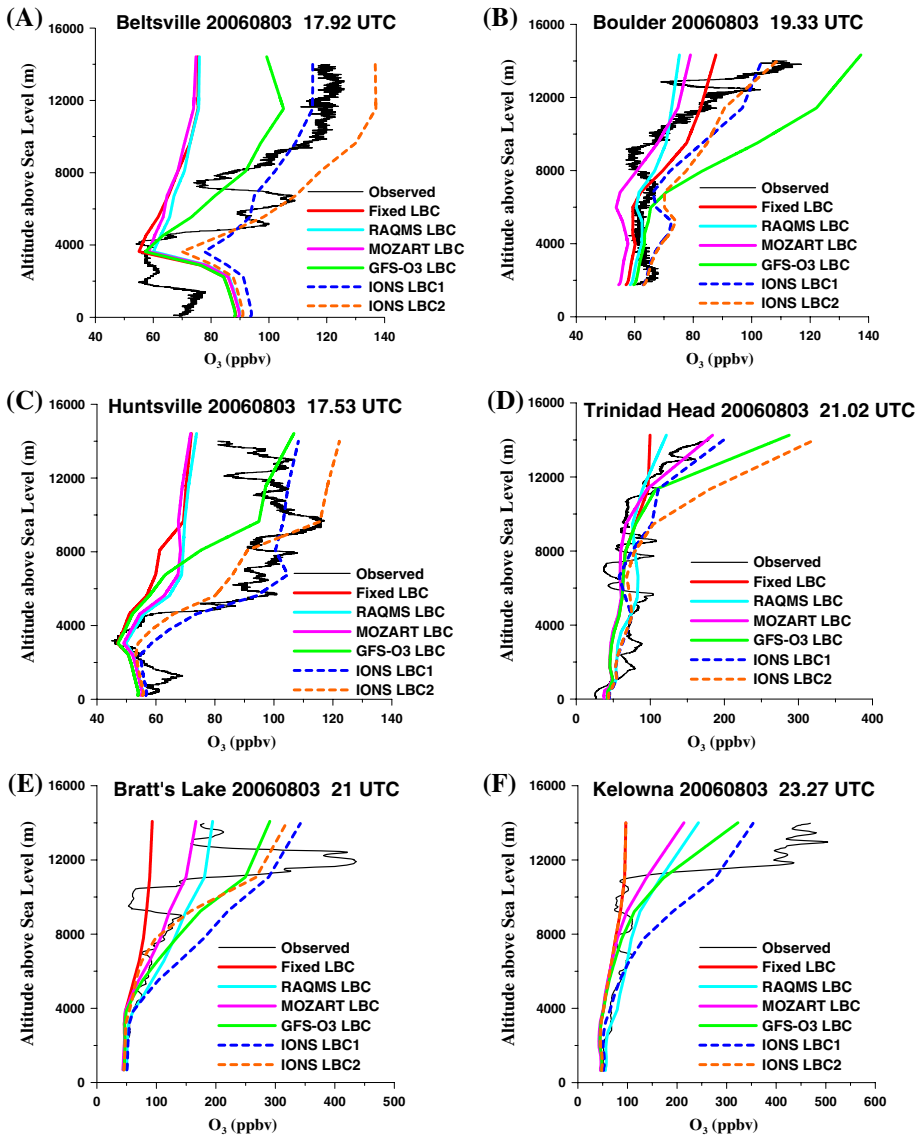


Fig. 3 The model simulations compared to IONS ozonesonde measurements at Beltsville (39.0°N, 76.5°W), Boulder (40.3°N, 105.2°W), Huntsville (35.3°N, 86.6°W), Trinidad Head (40.8°N, 124.2°W), Bratt's Lake (50.2°N, 104.7°W) and Kelowna (49.9°N, 119.4°W) on August 3, 2006

157 changing LBCs significantly affected the prediction at Bratt's Lake. However, none of these
 158 simulations could replicate the ozone peak values above 12 km altitude at Bratt's Lake and
 159 Kelowna. On August 3 at Kelowna, the northern boundary was the major inflow boundary
 160 (Fig. 4), which is also reflected by IONS-LBC2 results similar to the fixed LBC.

161 Figure 4 shows a spatial comparison of the relative change in O₃ prediction aloft (e.g.,
 162 ~9.6 km above ground level, the CMAQ's 20th layer) for each of the simulations compared
 163 with the time-invariant LBCs. Figure 4a shows that using the fixed LBCs rarely leads to

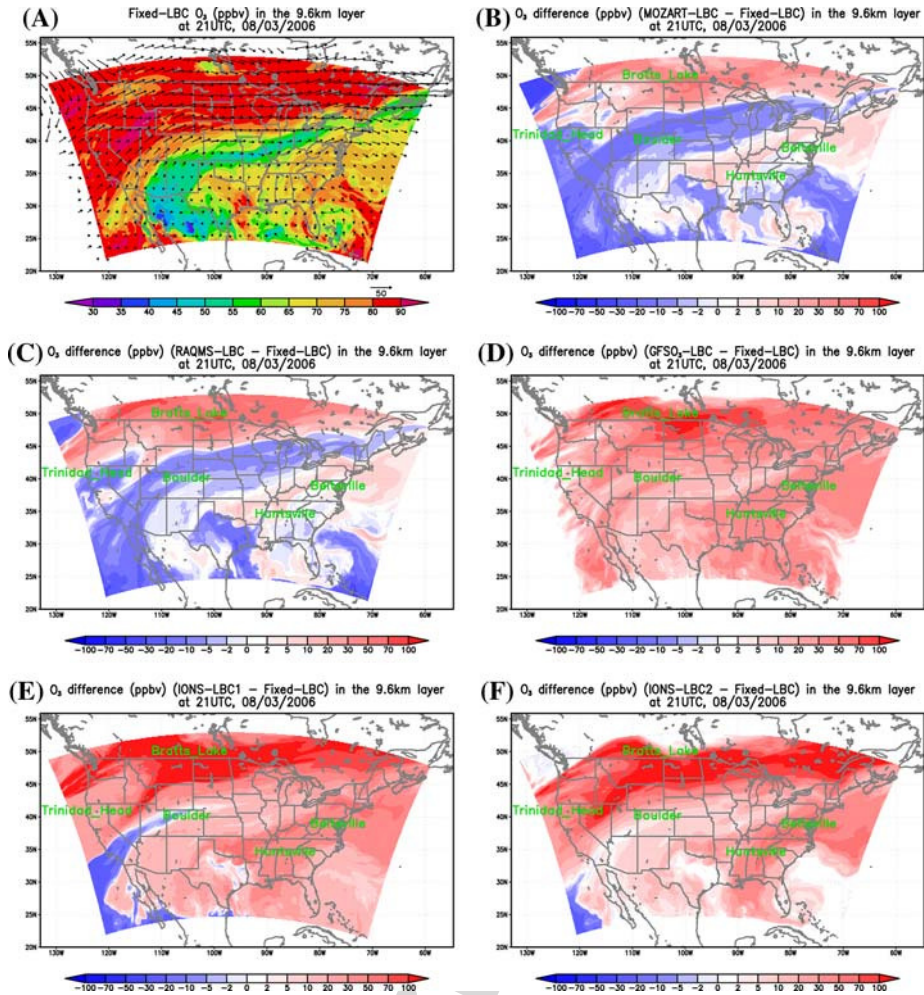


Fig. 4 Model simulated ozone (a for Fixed-LBC) and their differences (b–f) in the model’s 9.6km layer at 21Z, August 3, 2006

164 a prediction of more than 90ppbv aloft anywhere in the domain, though the ozonesondes
 165 in Fig. 3 (which are distributed throughout the simulation domain) have strong variations
 166 (50 ~ 500ppbv) at that altitude and above. Figure 4b and c show that using the chemical
 167 LBCs from MOZART and RAQMS results in large reductions of O₃ aloft, particularly south
 168 of the jet stream (refer to Fig. 4a) and in the subtropical regions as compared to the simulation
 169 using fixed LBC. MOZART and RAQMS LBCs have lower O₃ than the Fixed LBCs (Fig. 2)
 170 aloft along the western boundary (south of the jet stream) but higher O₃ along the northern
 171 boundary. Figure 4d shows that in most areas of continental United States, the GFS O₃ LBC
 172 increases O₃ prediction aloft compared with using Fixed LBCs, which is a direct result of
 173 increasing the O₃ on the lateral boundaries (Fig. 2). The two simulations with IONS LBCs
 174 (Fig. 4e, f) increase the O₃ predictions by more than 100ppbv (compared with the Fixed
 175 LBCs) in a swath along the jet stream from the western boundary across the northern portion

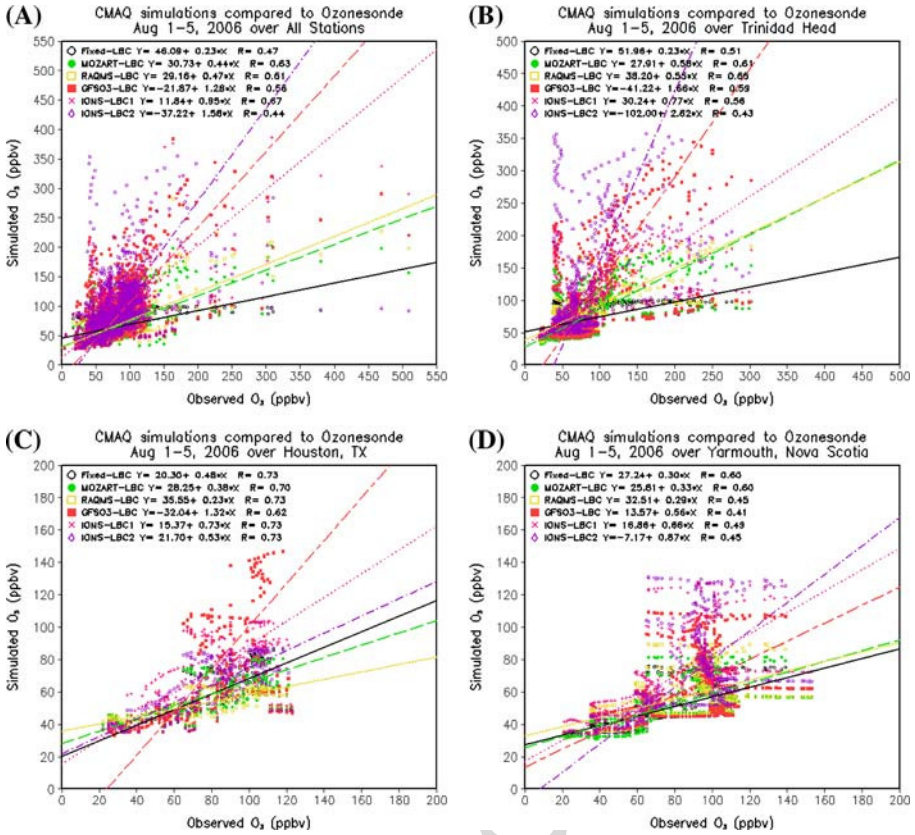


Fig. 5 The correlations between the simulations and measurement over IONS stations from August 1 to 5, 2006

176 of the domain. As noted above, this increase in O₃ aloft is consistent with measurements at
 177 Bratt’s Lake (Fig. 3e). The IONS LBCs correctly reduce the O₃ aloft in the southwestern
 178 USA, since the LBCs from IONS data use have relatively lower ozone observed in Table
 179 Mountain (not shown). The increases in O₃ prediction aloft and north of 40°N emanate from
 180 the western boundary in this event (compare Fig. 4e, f) since IONS LBC2 has the same
 181 northern boundary values as the Fixed LBC but uses ozonesonde data along the western
 182 boundaries.

183 Figure 5 compares observed and predicted O₃ values throughout the troposphere for the
 184 six simulations at the 15 IONS ozonesonde sites (Fig. 1) during 1–5 August 2006. The
 185 IONS-LBC1 simulation has the highest correlation coefficient R in Fig. 5a, which suggests
 186 that the observed profiles can provide valuable influences along lateral boundaries. The
 187 IONS-LBC2 case tends to overpredict O₃ in the mid-troposphere (Fig. 3) and has a lower
 188 correlation coefficient. The O₃ overprediction of IONS-LBC2 compared with IONS-LBC1
 189 over Trinidad head (Fig. 5b) reflects the result difference of using linear interpolation versus
 190 segmented assignment along the west boundary. The major overprediction of IONS-LBC2
 191 compared to IONS-LBC1 occurred above 9 km over Trinidad Head (Fig. 3d), which was
 192 caused by their difference along the western boundary (Fig. 4e, f). However, since we only
 193 have three stations along the west coast, more studies are needed to evaluate which method

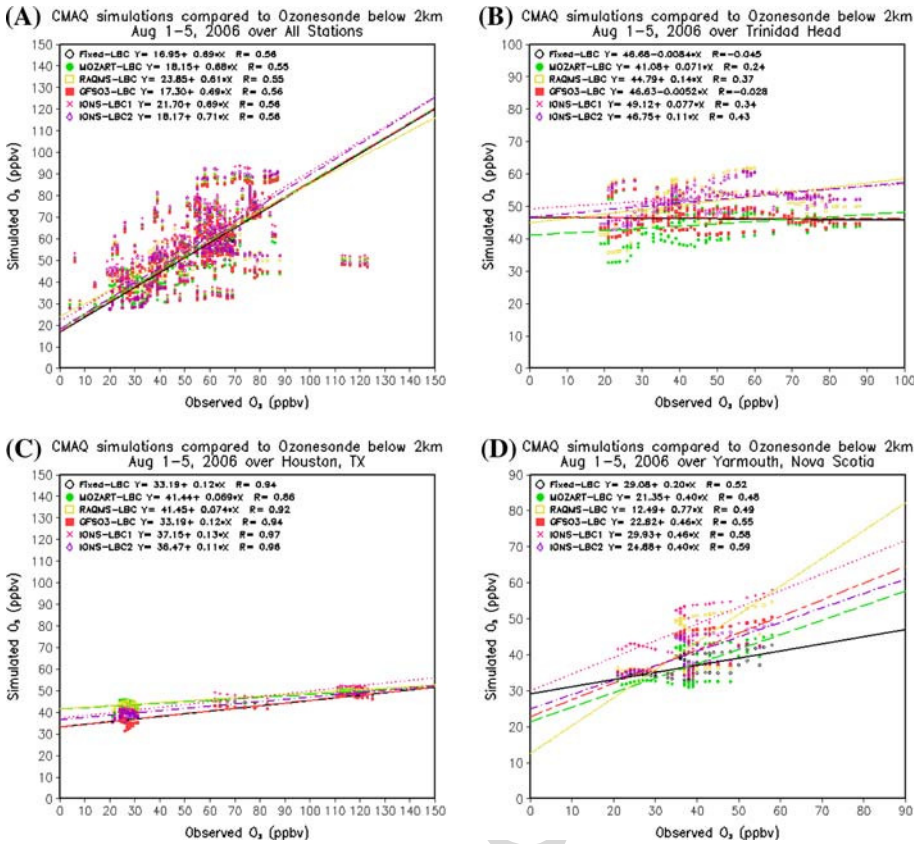


Fig. 6 Same as Fig. 5 but only for the altitudes below 2 km

194 is better for using ozonesonde data. Among the simulations using global model LBCs, the
 195 MOZART and RAQMS LBCs yielded similar correlations, and the GFS-O₃ LBC had the
 196 more reasonable regression slope, reflecting its skill for predicting O₃ variability aloft. The
 197 simulation with the Fixed LBCs yielded the lowest prediction skill for O₃ variations in the
 198 upper troposphere, as expected, as seen by its low regression slope (0.23 for all stations). In
 199 the lower troposphere (i.e., below 2 km), the differences between the simulations are small
 200 (Fig. 6). Therefore, in general, varying the LBCs most directly affects the O₃ concentrations
 201 in the middle and upper troposphere, but over time the specification of the LBCs can influence
 202 the surface O₃ concentrations on the interior of the forecast domain through transport and
 203 vertical advection processes (e.g., due to convection). Near the surface, regional or local
 204 emissions often play a more important role in dictating day-to-day O₃ prediction. However,
 205 the relative importance of each influencing factor also depends on the locations and scenarios.
 206 For instance, using time-varying LBCs from RAQMS improved all-altitude and low-altitude
 207 O₃ prediction at Trinidad Head (Figs. 5b, 6b) because it is located near the western boundary
 208 of the domain (Fig. 1) and it was used in the specification of the O₃ concentrations along the
 209 western boundary. On the other hand, the LBCs derived from global models did not show
 210 significant improvement over Houston at high altitudes (except for GFS O₃ that has better
 211 slope) or low altitudes (Figs. 5c, 6c). The use of time-varying LBCs had a moderate impact

at Yarmouth, Nova Scotia, (Figs. 5d, 6d) as it is located in the northeastern quadrant of the NAQFG domain (close to Eastern and Northern outflow boundaries). The use of real-time global-model LBCs and IONS LBCs yielded better regression slopes over Yarmouth, but did not show an advantage in term of the correlation coefficient (Figs. 5d, 6d).

4 Comparison to surface observations

In the NAQFG, verification with surface measurements is a primary performance indicator because the target forecasts are for near-surface O₃, which most directly affects the human population. The Environmental Protection Agency’s Air Quality System (AQS) (available from <http://www.epa.gov/air/data/aqsdb.html>; <http://airnow.gov>) network provides hourly surface ozone measurement across the United States and largely in urban areas, where the human population is concentrated. During this period, NAQFG surface O₃ prediction had a high bias, and using global LBCs may exaggerate the NAQFG overprediction of O₃ (Lee et al., this issue). In this study, 1635 AQS/AIRNOW stations within the NAQFG domain are used for near-surface verification. Table 3 shows the statistical results for the hourly data over these surface stations. Global models and IONS lateral boundary conditions yield better regression slopes when compared against all AIRNOW sites, implying that these LBCs could improve the model prediction for ozone variation magnitudes, though these LBCs could cause higher mean biases. The impact of LBCs becomes more evident when the evaluation is limited to stations west of -115°W (i.e., near the western boundary of the domain). Figure 7 shows the surface O₃ mean biases for the six simulations superimposed on their predicted mean O₃ (for Fixed LBCs only) or on mean predicted O₃ differences from Fixed LBCs (all other simulations). The use of MOZART LBCs shows the best improvement relative to the Fixed LBCs in this region by reducing the mean bias in surface O₃ by 2.5 ppbv and increasing the correlation coefficient/slope (Table 3). The most significant improvement occurred in Pacific Northwest and California coastal regions (Fig. 7b). The RAQMS LBCs simulation has

Table 3 CMAQ simulations compared to AIRNOW hourly O₃ data from August 1 to 5

	All stations	West of -115°W	North of 43°N	East of -85°W
Fixed LBC	S=0.887 R=0.714 MB=8.0 ppbv	S=0.804 R=0.691 MB=4.7 ppbv	S=0.873 R=0.737 MB=7.5 ppbv	S=0.844 R=0.742 MB=11.3 ppbv
RAQMS LBC	S=0.911 R=0.718 MB=10.0 ppbv	S=0.914 R=0.703 MB=7.1 ppbv	S=0.942 R=0.742 MB=10.0 ppbv	S=0.823 R=0.744 MB=12.8 ppbv
MOZART LBC	S=0.941 R=0.716 MB=8.2 ppbv	S=0.872 R=0.730 MB=2.2 ppbv	S=0.985 R=0.743 MB=6.9 ppbv	S=0.872 R=0.737 MB=11.8 ppbv
GFS O ₃ LBC	S=0.935 R=0.714 MB=9.2 ppbv	S=0.820 R=0.697 MB=4.8 ppbv	S=0.922 R=0.724 MB=9.0 ppbv	S=0.858 R=0.736 MB=12.9 ppbv
IONS LBC1	S=0.947 R=0.718 MB=12.4 ppbv	S=0.912 R=0.692 MB=10.4 ppbv	S=0.905 R=0.709 MB=12.9 ppbv	S=0.817 R=0.742 MB=15.3 ppbv
IONS LBC2	S=0.952 R=0.723 MB=10.1 ppbv	S=0.910 R=0.698 MB=9.0 ppbv	S=0.922 R=0.736 MB=9.2 ppbv	S=0.858 R=0.742 MB=13.0 ppbv

S is regression slope; R is correlation coefficient; MB is mean bias

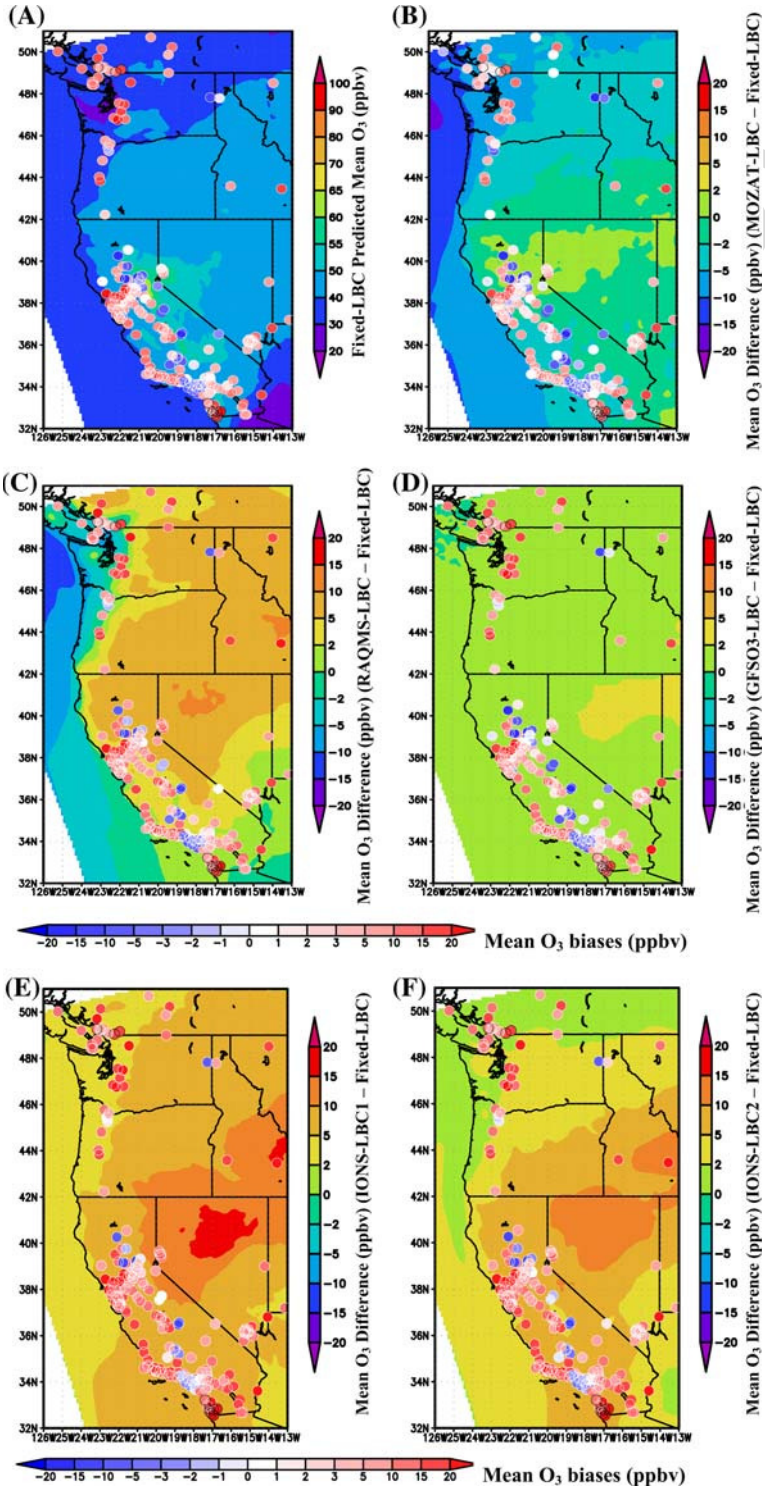
Author Proof

Fig. 7 Mean surface O₃ prediction (plot **a** for Fixed LBC), mean O₃ prediction differences (**b** for MOZART LBC, **c** for RAQMS LBC, **d** for GFS O₃ LBC, **e** for IONS LBC1 and **f** for IONS LBC2) and their mean biases from AIRNOW observations during August 1 to 5, 2006

the best regression slope, but it also tends to increase the mean bias (Table 3). It should be noted that the greatest impact from the RAQMS LBCs occurred not along the coast but further inland in Idaho (Fig. 7c). The simulations with IONS LBC also show similar features. It could be caused by overpredictions of PBL height and the corresponding vertical mixing as indicated by Lee et al. (this issue) that WRF-NMM/CMAQ tends to overpredict PBL height for the 2006 simulations. Overpredicted PBL can bring high ozone from middle layers to surface while RAQMS and IONS LBCs have higher ozone concentration between 2 and 6 km along the western boundary than that in MOZART (Fig. 1). The impact of GFS O₃ LBC near surface is relatively small over this region since it is used only above 11 km and needs longer transport time/distance to affect surface ozone (Table 3; Fig. 7d). The GFS O₃ LBC simulation has a stronger impact in the region north of 43°N. The two IONS LBCs simulations resulted in the highest surface O₃ bias over the whole domain (Table 3). Along the west coast, the differences between two IONS LBCs and the fixed LBCs range from 0 to 10 ppbv (Fig. 7e, f). Near the western boundary, all of the time-varying LBCs improve the regression slopes relative to the fixed LBCs, but only the MOZART LBC reduces the mean bias and has the highest correlation coefficient/slope. Table 3 also shows the statistical comparison of surface O₃ predictions over the eastern United States. The LBC influence in east coast during this period is relatively insignificant since it is the prevailing outflow region. In east coast, the simulations with various LBCs did not show significant difference for O₃ prediction on the correlation statistics while the mean biases are less than 4 ppbv. So the LBCs mainly affect the background concentration of predicted ozone, not its variation, as the variation and gradient from western and northern inflow boundaries have been diffused during the long-distance transport to the east coast.

5 Conclusion

This study compares the impacts on tropospheric ozone prediction over continental United States from using various LBCs derived from global models and from ozonesondes. Although this period is not a noticeable intrusion event, these boundary conditions still show a strong impact on ozone prediction at most altitudes. Depending on locations and scenarios, the simulations with these LBCs did not always yield better results than that with the fixed LBCs. For global-model LBCs, the error could be caused by global model performance or CMAQ regional prediction. When ozonesonde LBCs are used, CMAQ performance depends on ozonesonde location relative to the regional-model boundary locations, spatial/temporal resolutions, the treatment of ozonesonde data and how CMAQ evolves the observed information. Lee et al. [13] showed that high ozone aloft can often be mixed downward too quickly by CMAQ, thereby increasing model errors in the lower troposphere. In this study, we found a similar behavior: the simulation with IONS LBC1 shows good agreement with 15 IONS ozonesonde data aloft, but leads to O₃ overestimation near surface. The performance inconsistency implies that CMAQ could overestimate the vertical mixing and bring too much ozone downward. This problem could be related to the operational CMAQ's coarse vertical resolution in the free troposphere (with top layer's thickness of 4 km). The operational CMAQ uses only 22 vertical layers for computation efficiency. This relatively coarse vertical resolution could not resolve the tropopause boundary, and erroneously mix too much stratospheric ozone into the free troposphere. In lower troposphere, boundary layer mixing can



280 also transfer the ozone to the surface [13]. We are investigating this issue. The ozonesonde
281 site locations can be far from the domain boundaries, which introduces additional possible
282 errors in IONS LBCs simulations. Current 15 IONS ozonesonde sites are not sufficient for
283 LBCs due to their spatial and temporal resolution, though the preliminary test in IONS LBC1
284 shows encouraging results in middle and upper troposphere.

285 At high altitudes, ozone predictions are mainly related to stratospheric influence, in which
286 using GFS O₃ for LBCs and ozonesonde-derived LBCs can capture strong transport events,
287 perhaps due in part to their high spatial resolution. For some events, GFS O₃ also tends to
288 overpredict upper-troposphere ozone, possibly due to insufficient vertical resolution of assi-
289 milated SBUV-2 satellite data. In this study, we did not test the use of global simulations for
290 the top boundary condition [32], or use potential vorticity as the indicator of stratosphere–
291 troposphere exchange, which could yield even stronger impacts on upper atmospheric pre-
292 diction. Compared to GFS O₃ LBC, RAQMS and MOZART can provide height-resolved
293 LBCs for additional species. These species include long-lifetime CO and NO_y, which can
294 be transported from distant sources and possibly affect regional ozone production. In some
295 events, such as the biomass burning near the domain boundary, very active species, like NO_x,
296 could also cause great impacts. The chemical transformation of LBCs needs to be evaluated
297 in the future.

298 This study demonstrated the potential for using time-varying chemical LBCs for air qua-
299 lity predictions of tropospheric O₃. The gains in skill from using LBCs derived from global
300 models are promising. Although each of the global models used in this study has different
301 strengths, it is clear that time-varying chemical LBCs derived from those models can contri-
302 bute toward improved simulations of O₃ above the surface layer compared to simulation
303 with fixed profile LBCs. Additional simulations should be conducted with more represen-
304 tative values for the fixed profile LBCs (particularly in the upper troposphere) to determine
305 the full advantage of using chemical LBCs from global models. However, even if the time-
306 invariant LBCs are increased aloft, only LBCs derived from daily conditions can capture
307 the transient pollutant events that are critical to predicting air quality over a long period. In
308 addition, this study shows that the LBCs derived from ozonesonde measurements yielded
309 more skillful O₃ predictions, particularly in the upper troposphere. While we recognize that
310 the NAQFG cannot use these data in real time because they are not centrally reported, this
311 study can advocate the assembly and reporting of a real-time 3D air quality network that
312 could be used, in part, to improve air quality predictions. Finally, this study has highlighted
313 how improvements in global air quality models could yield better results for regional air qua-
314 lity prediction. Lateral boundary conditions are essential for regional air quality prediction,
315 even for the scenario without strong intrusions. However, once the regional air quality model
316 adopts the global-model LBCs, uncertainties from the global models could impact errors
317 in the regional predictions, and we may need to overcome more uncertain factors than the
318 regional models do to achieve improvement.

319 **Acknowledgements** The IONS ozonesonde data, which was supported by NASA's INTEX project within
320 the Tropospheric Chemistry Program (B. G. Doddridge and J. H. Crawford). EPA AIRNOW program staff
321 provided the observations necessary for quantitative model evaluation.

322 References

- 323 1. Byun DW, Schere KL (2006) Review of the governing equations, computational algorithms, and other
324 components of the Models-3 Community Multiscale Air Quality (CMAQ) modeling system. *Appl Mech*
325 *Rev* 59:51–77

- 326 2. Chen F, Dudhia J (2001) Coupling an advanced land-surface/hydrology model with the Penn State/NCAR
 327 MM5 modeling system. Part I: model description and implementation. *Mon Wea Rev* 129:569–585
 328 3. Ferrier BS, Jin Y, Lin Y, Black T, Rogers E, DiMego G (2002) Implementation of a new grid-scale
 329 cloud and precipitation scheme in the NCEP Eta model. Preprints, 15th conference on numerical weather
 330 prediction, San Antonio, TX, American Meteorological Society, pp 280–283
 331 4. Gery MW, Whitten GZ, Killus JP, Dodge MC (1989) A photochemical kinetics mechanism for urban
 332 and regional scale computer modeling. *J Geophys Res* 94:925–956
 333 5. Granier C et al (2004) Present and future surface emissions of atmospheric compounds. Rep EVK
 334 2199900011, Eur Comm, Brussels
 335 6. Horowitz LW et al (2003) A global simulation of tropospheric ozone and related tracers: description and
 336 evaluation of MOZART, version 2. *J Geophys Res* 108(D24):4784. doi:10.1029/2002JD002853
 337 7. Jacob DJ, Logan JA, Murti PP (2001) Effect of rising Asian emissions on surface ozone in the United
 338 States. *Geophys Res Lett* 26(14):2175–2178
 339 8. Jaffe D, Price H, Parrish D, Goldstein A, Harris J (2003) Increasing background ozone during spring on
 340 the west coast of North America. *Geophys Res Lett* 30(12)
 341 9. Janjic Z (1994) The Step-Mountain Eta coordinate model: further developments of the convection, viscous
 342 sublayer, and turbulence closure schemes. *Mon Wea Rev* 92:927–945
 343 10. Janjic ZI (2002) Nonsingular implementation of the Mellor–Yamada level 2.5 Scheme in the NCEP Meso
 344 model. NCEP Office Note, No. 437, 61 pp
 345 11. Janjic ZI (2003) A nonhydrostatic model based on a new approach. *Meteor Atmos Phys* 82:271–285
 346 12. Kondragunta S, Lee P, McQueen J, Kittaka C, Prados A, Ciren P, Laszlo I, Pierce B, Hoff R, Szykman J
 347 (2008) Air quality forecast verification using satellite data. *J Appl Meteor Climatol*, in press
 348 13. Lee P, McKeen S, McQueen J, Kang D, Tsidulko M, Lu S, Lin H-M, DiMego G, Seaman N, Davidson P
 349 (2007) Air quality forecast using WRF/MMM-CMAQ during the TexAQS. Preprints, 9th conference on
 350 Atmos. Chem./, American Meteorological Society, San Antonio, TX, 15–18, Jan 2007, pp 1–6
 351 14. Lee PC, Kang D, McQueen J, Tsidulko M, Hart M, DiMego G, Seaman N, Davidson P (2008) Impact of
 352 domain size on modeled ozone forecasts for the Northeastern US. *J Appl Meteor Climatol* 47(2):443–461
 353 15. Lee PS et al (this issue) Impact of consistent boundary layer mixing approaches between NAM and
 354 CMAQ, submitted to *Environ Fluid Mech* (CMAS special issue)
 355 16. McLinden CA, Olsen SC, Hannegan B, Wild O, Prather MJ (2000) Stratospheric ozone in 3-D models:
 356 a simple chemistry and the cross-tropopause flux. *J Geophys Res* 105(D11):14,653–14,665
 357 17. Moorathi S, Iredell M (1998) Prognostic ozone: changes to the 1998 NCEP operational MRF model
 358 analysis/forecast system: the use of TOVS level 1-b radiances and increased vertical diffusion. Available
 359 at <http://www.nws.noaa.gov/om/tpb/449.htm> from the National Weather Service, Office of Meteorology,
 360 1325 East-West Highway, Silver Spring, MD 20910
 361 18. NCEP (2004) GFS—Global data assimilation. Available at <http://www.emc.ncep.noaa.gov/gmb/gdas/>
 362 19. Newchurch MJ, Ayoub MA, Oltmans S, Johnson B, Schmidlin FJ (2003) Vertical distribution of ozone
 363 at four sites in the United States. *J Geophys Res* 108(D1):4031. doi:10.1029/2002JD002059
 364 20. Otte TL, Pouliot G, Pleim JE, Young JO, Schere KL, Wong DC, Lee PCS, Tsidulko M, McQueen JT,
 365 Davidson P, Mathur R, Chuang H-Y, DiMego G, Seaman NL (2005) Linking the Eta model with the
 366 Community Multiscale Air Quality (CMAQ) modeling system to build a national air quality forecasting
 367 system. *Wea Forecast* 20:367–384
 368 21. Pfister G, Hess PG, Emmons LK, Lamarque J-F, Wiedinmyer C, Edwards DP, Pétron G, Gille JC, Sachse
 369 GW (2005) Quantifying CO emissions from the 2004 Alaskan wildfires using MOPITT CO data. *Geophys*
 370 *Res Lett* 32:L11809. doi:10.1029/2005GL022995
 371 22. Pierce T, Geron C, Bender L, Dennis R, Tonnesen G, Guenther A (1998) Influence of increased isoprene
 372 emissions on regional ozone modeling. *J Geophys Res* 103:25611–25629
 373 23. Pierce RB, Al-Saadi JA, Schaack T, Lenzen A, Zapotocny T, Johnson D, Kittaka C, Buker M, Hitch-
 374 man MH, Tripoli G, Fairlie TD, Olson JR, Natarajan M, Crawford J, Fishman J, Avery MA, Browell
 375 EV, Creilson J, Kondo Y, Sandholm ST (2003) Regional Air Quality Modeling System (RAQMS) pre-
 376 dictions of the tropospheric ozone budget over east Asia. *J Geophys Res* 108(D21):8825. doi:10.1029/
 377 2002JD003176
 378 24. Pierce RB, Schaack T, Al-Saadi JA, Fairlie TD, Kittaka C, Lingenfelter G, Natarajan M, Olson J, Soja
 379 A, Zapotocny T, Lenzen A, Stobie J, Johnson D, Avery MA, Sachse GW, Thompson A, Cohen R, Dibb
 380 JE, Crawford J, Rault D, Martin R, Szykman J, Fishman J (2007) Chemical data assimilation estimates
 381 of continental US ozone and nitrogen budgets during the intercontinental chemical transport experiment-
 382 North America. *J Geophys Res* 112(D12S21). doi:10.1029/2006JD007722
 383 25. Pleim JE (2007) A combined local and nonlocal closure model for the atmospheric boundary layer. Part
 384 I: model description and testing. *J Appl Meteor Climatol* 46:1383–1395

- 385 26. Pleim JE, Xiu A, Finkelstein PL, Otte TL (2001) A coupled land-surface and dry deposition model and
386 comparison to field measurements of surface heat, moisture, and ozone fluxes. *Water Air Soil Pollut Focus*
387 1:243–252
- 388 27. Rood R, Douglas AR, Kaye JA, Geller MA, Chen CY, Allen DJ, Larsen EM, Nash ER, Nielsen
389 JE (1991) Three-dimensional simulations of wintertime ozone variability in the lower stratosphere. *J*
390 *Geophys Res* 96(D3):5055–5071
- 391 28. Stobie JM (1985) The use of optimum interpolation at AFGWC. Paper presented at 7th conference on
392 numerical weather prediction. American Meteorological Society, Montreal, Que., Canada
- 393 29. Stobie JM (2000) Algorithm theoretical basis document for statistical digital filter (SDF) analysis system
394 (stretch-grid version). Data Assim. Off., NASA Goddard Space Flight Cent., Greenbelt, MD
- 395 30. Streets DG, Bond TC, Carmichael GR, Fernandes SD, Fu Q, He D, Klimont Z, Nelson SM, Tsai NY,
396 Wang MQ, Woo J-H, Yarber KF (2003) An inventory of gaseous and primary aerosol emissions in Asia
397 in the year 2000. *J Geophys Res* 108(D21):8809. doi:[10.1029/2002JD003093](https://doi.org/10.1029/2002JD003093)
- 398 31. Tang Y, Carmichael GR, Horowitz LW, Uno I, Woo J-H, Streets DG, Dabdub D, Kurata G, Sandu A,
399 Allan J, Atlas E, Flocke F, Huey LG, Jakoubek RO, Millet DB, Quinn PK, Roberts JM, Williams EJ,
400 Nowak JB, Worsnop DR, Goldstein A, Donnelly S, Schaubfler S, Stroud V, Johnson K, Avery MA, Singh
401 HB, Apel EC (2004) Multi-scale Simulations of Tropospheric Chemistry in the Eastern Pacific and US
402 West Coast during Spring 2002. *J Geophys Res* 109:D23S11. doi:[10.1029/2004JD004513](https://doi.org/10.1029/2004JD004513)
- 403 32. Tang Y, Carmichael GR, Thongboonchoo N, Chai T, Horowitz LW, Pierce RB, Al-Saadi JA, Pfister G,
404 Vukovich JM, Avery MA, Sachse GW, Ryerson TB, Holloway JS, Atlas EL, Flocke FM, Weber RJ,
405 Huey LG, Dibb JE, Streets DG, Brune WH (2007) Influence of lateral and top boundary conditions on
406 regional air quality prediction: a multiscale study coupling regional and global chemical transport models.
407 *J Geophys Res* 112:D10S18. doi:[10.1029/2006JD007515](https://doi.org/10.1029/2006JD007515)
- 408 33. Thompson AM, Stone JB, Witte JC, Miller SK, Oltmans SJ, Kucsera TL, Ross KL, Pickering KE, Merrill
409 JT, Forbes G, Tarasick DW, Joseph E, Schmidlin FJ, McMillan WW, Warner J, Hints EJ, Johnson
410 JE (2007) Intercontinental chemical transport experiment ozonesonde network study (IONS) 2004:1.
411 Summertime upper troposphere/lower stratosphere ozone over northeastern North America. *J Geophys*
412 *Res* 112:D12S12. doi:[10.1029/2006JD007441](https://doi.org/10.1029/2006JD007441)
- 413 34. Thompson AM, Yorks JE, Miller SK, Witte JC, Dougherty KM, Morris GA, Baumgardner D, Ladino L,
414 Rappenglueck B (2008) Free tropospheric ozone sources and wave activity over Mexico City and Houston
415 during MILAGRO/Intercontinental Transport Experiment (INTEXB) Ozonesonde Network Study, 2006
416 (IONS-06). *Atmos Chem Phys Discuss* 8:5979–6007
- 417 35. van der Werf GR, Randerson JT, Giglio L, Collatz GJ, Kasibhatla PS, Arellano AF Jr (2006) Interannual
418 variability in global biomass burning emissions from 1997 to 2004. *Atmos Chem Phys* 6:3423–3441